# Automated quantification of lipid storage induced by glucocorticoid signaling in BMSC-derived osteoblasts

Colby Gross[1], Husam Bensreti[1], Meghan E. McGee-Lawrence[1]
[1]Medical College of Georgia, Augusta University, Augusta, GA. **Disclosures:** MM-L: ORS Board of Directors [9]

INTRODUCTION: Glucocorticoids (GCs) are released from the adrenal cortex in a circadian manner and during stress to regulate tissue metabolic activity. GCs can bind either glucocorticoid receptors (GR) or mineralocorticoid receptors (MR), which then act as transcription factors to mediate downstream signaling effects. We previously demonstrated aberrant GC-induced intracellular lipid accumulation within osteoblasts derived from aged bone marrow stromal cells (BMSCs), driven at least in part by a net upregulation of genes related to lipid storage (e.g., Perilipin1, Cidec), but the relative contributions of the GR and MR were unclear in this process [1]. Later studies suggested that genetically deleting the GR exacerbated (rather than protected against) this lipid storage phenomenon, whereas targeting the MR in GR-deficient osteoblasts via non-specific pharmacological inhibitors effected a partial rescue [2]. Here, we report the effects of two experimental GR/MR inhibitors on lipid storage by BMSC-derived osteoblasts using a novel, automated method for quantifying intracellular lipid storage in vitro. This automated methodology was developed with the goals of decreasing error, measurement time, and both intra- and inter-observer variability related to subjectivity in the manual measurement and imaging procedures used in previous studies [1,2].

METHODS: Outbred CD-1 mice (12 weeks old, female) were obtained from a commercial supplier (Envigo). BMSC were isolated using established procedures [1,2] and cultured for 14 or 21 days in osteogenic media with or without the GC dexamethasone (Dex). Cells were fixed and stained with Oil Red O (ORO) to detect lipids and Hoechst to highlight the nucleus (for accurate quantification of total cell number). In a subset of studies, mineralized matrix was detected using alizarin red staining, as previously reported [1]. Automated imaging and quantification were performed using a Cytation 5 plate reader and Gen5 software (Agilent BioTek). A linear regression model comparing automated and manual quantification was used to select the fluorescence intensity threshold for ORO detection. To further validate this new automated quantification methodology in a previously established mouse model, BMSC from 6 mo old Osx-Cre: GR conditional knockout (GR- CKOosx) and WT littermates [2] were cultured in osteogenic media in the presence of Dex and either the GR-specific inhibitor Relacorilant (RELA) or the co-GR/MR targeting drug Miricorilant (MIRI) for 14 or 21 days. Data were analyzed using one-factor ANOVA and t-tests for post hoc comparisons between groups (JMP Pro 16).

RESULTS: Preliminary experiments designed to optimize seeding density for automated quantification of osteoblastic lipid storage showed that seeding densities of $4x10^6$ cells/well in 12-well plates (i.e., $1.14 \times 10^6$ cells/cm$^2$), used previously [2], impaired detection of discrete cell nuclei for accurate quantification of total cell numbers. Reducing seeding densities by half to $2x10^6$ cells/well (i.e., $0.57 \times 10^6$ cells/cm$^2$) improved detection methods substantially and showed no differences in total cell numbers detected as compared to manual quantification methods. Comparison between manual and automated quantification of ORO-containing osteoblasts showed no difference between the approaches ($p>0.806$); both methods demonstrated that Dex significantly increased the relative abundance of lipid-storing osteoblasts as compared to osteogenic media alone ($p=0.0003$, $p=0.0115$, respectively) as previously reported for manual quantification (Figure 1A, [1]). However, alizarin red staining of cultures at D21 after seeding revealed that the optimized seeding density of $2x10^6$ cells/well (i.e., $0.57 \times 10^6$ cells/cm$^2$) that facilitated accurate automated quantification of total cell number resulted in lower and more variable production of mineralized matrix. These results suggest that endpoints relating to osteoblastic lipid storage as compared to osteoblastic matrix production, when possible, should be quantified in separate experiments so that optimal seeding densities can be used for each endpoint separately. Automated analysis of intracellular lipid storage in BMSC-derived osteoblast cultures derived from GR-CKOosx mice revealed a 30% increase in ORO-containing osteoblasts as compared to WT cells, comparable to previous results obtained via manual quantification [2]. In pharmacological studies, the GR-specific antagonist Relacorilant increased lipid storage in WT cells by nearly 25% without causing further increases in GR-CKOosx cultures (Figure 1B) but surprisingly, the co-GR/MR antagonist Miricorilant was unable to rescue GC-induced lipid storage in BMSC-derived osteoblasts, which is in contrast with previous results obtained with MR-specific antagonists like eplerenone and spironolactone (Figure 1B).

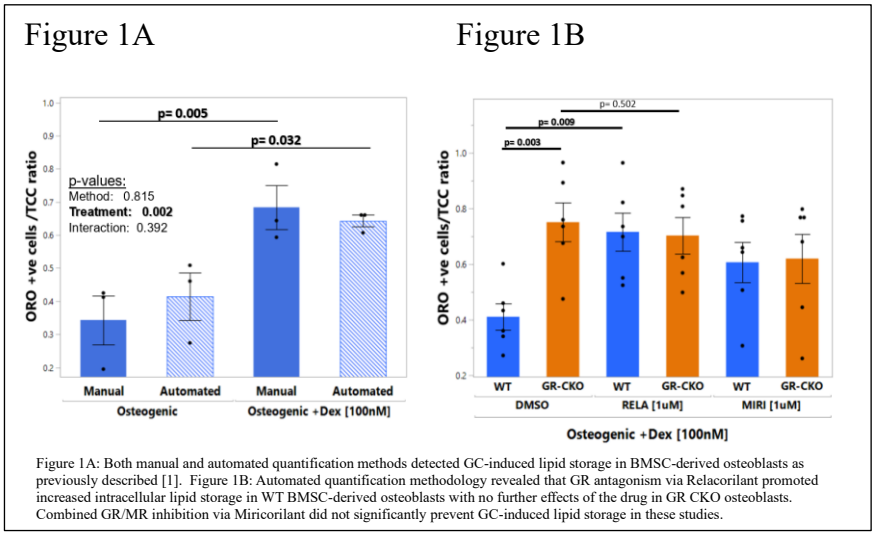


Figure 1A: Both manual and automated quantification methods detected GC-induced lipid storage in BMSC-derived osteoblasts as previously described [1]. Figure 1B: Automated quantification methodology revealed that GR antagonism via Relacorilant promoted increased intracellular lipid storage in WT BMSC-derived osteoblasts with no further effects of the drug in GR CKO osteoblasts. Combined GR/MR inhibition via Miricorilant did not significantly prevent GC-induced lipid storage in these studies.

DISCUSSION: Taken together, these data further support a role for GC-mediated signaling via GR and MR in mechanisms of osteoblast lipid storage and cellular metabolism, and importantly establish an unbiased, automated methodology for quantifying this phenomenon in ongoing and future studies. The automated methodology described here facilitates imaging and analysis of various fluorophore and brightfield channels, substantially reducing the time required to image and analyze experiments. Establishing a standardized, unbiased approach for quantification of lipid-storing cells is likely to enhance consistency and reliability by reducing intra- and inter-observer variability; however, these specific comparisons remain the subject of future studies as they have not yet been rigorously tested. Using automated quantification methodology, we demonstrated the ability to reproduce experimental trends previously assessed via manual quantification (i.e., enhanced GC-induced lipid storage in GR-CKOosx osteoblasts), and also tested the in vitro effects of two experimental GR and GR/MR antagonists in mechanisms of osteoblastic lipid storage. Pharmacological inhibition of GR with Relacorilant increased lipid storage in WT, but not GR-CKOosx, BMSC-derived osteoblasts supporting the relevance of GR-mediated signaling in maintaining normal osteoblastic lipid homeostasis. Interestingly, combined inhibition of MR and GR with Miricorilant did not significantly rescue this phenomenon, which is in contrast with the partial rescue of GC-induced lipid storage seen in GR-CKOosx osteoblasts treated with MR-specific antagonists like eplerenone and spironolactone [2]. However, additional replicates and further studies need to be performed with MR-specific antagonists, using comparable automated quantification methodology, to fully define the roles of GR and MR in osteoblastic lipid storage, cellular metabolism, and cellular dysfunction during aging.

SIGNIFICANCE/CLINICAL RELEVANCE: These findings support the idea that GC-induced signaling via GR and/or MR may be a key regulator of osteoblastic function during aging, and establish a novel, unbiased method for investigation of intracellular lipid storage in this mechanism in future studies.

ACKNOWLEDGEMENTS: National Institutes on Aging Grant Number(s): P01-AG036675 (Project 4)
REFERENCES: [1] McGee-Lawrence et al., J Bone Miner Res 31: 116-128. (2016) [2] Pierce et al., J Bone Miner Res 37: 285-302. (2022). IMAGES: Fig 1.